

Biocatalytic site- and enantioselective oxidative dearomatization of phenols

Summer A. Baker Dockrey^{1,2}, April L. Lukowski^{2,3}, Marc R. Becker¹ and Alison R. H. Narayan^{1,2,3*}

The biocatalytic transformations used by chemists are often restricted to simple functional-group interconversions. In contrast, nature has developed complexity-generating biocatalytic reactions within natural product pathways. These sophisticated catalysts are rarely employed by chemists, because the substrate scope, selectivity and robustness of these catalysts are unknown. Our strategy to bridge the gap between the biosynthesis and synthetic chemistry communities leverages the diversity of catalysts available within natural product pathways. Here we show that, starting from a suite of biosynthetic enzymes, catalysts with complementary substrate scope as well as selectivity can be identified. This strategy has been applied to the oxidative dearomatization of phenols, a chemical transformation that rapidly builds molecular complexity from simple starting materials and cannot be accomplished with high selectivity using existing catalytic methods. Using enzymes from biosynthetic pathways, we have successfully developed a method to produce *ortho*-quinol products with controlled site- and stereoselectivity. Furthermore, we have capitalized on the scalability and robustness of this method in gram-scale reactions as well as multi-enzyme and chemoenzymatic cascades.

Oxidative dearomatization of phenolic compounds is a powerful transformation for the synthesis of complex molecules, providing an avenue for simultaneously introducing stereochemical information and generating products that are primed for further reaction¹. For example, chemical methods exist for the conversion of simple phenols to dearomatized products, with concomitant formation of new C–C, C–N, C–halogen and C–O bonds². A number of reagents for dearomatization to afford *ortho*-quinol products (**2**, Fig. 1a)^{3–5}, including I^{III}, I^V, Pb^{IV} and Cu^I, have been developed and leveraged for the chemical synthesis of a range of bioactive natural products (Fig. 1b)^{1,4,6–8}. However, in addition to the requirement for stoichiometric amounts of these reagents, two major challenges associated with these chemical methods are site-selectivity and product stability. For example, highly substituted resorcinol substrates such as **3** are chemically oxidized to afford mixtures of isomers such as **4**, **5** and **6**, which can fragment to afford quinone products (**11**, Fig. 1c)⁹. Furthermore, the desired quinol products are often difficult to use productively, because side reactions such as dimerization¹⁰ (**7**), rearomatization^{11,12} (**8**, **9** and **10**) and rearrangement¹³ are facile under the requisite reaction conditions. Moreover, the development of asymmetric catalytic versions of these oxidative dearomatizations has proven challenging, particularly for cases involving concomitant C–O bond formation (**1**→**2**, Fig. 1a)¹⁴. Although high enantioselectivities have been achieved with stoichiometric amounts of chiral hypervalent iodine reagents, superstoichiometric chiral metal complexes⁴ and in cases where intramolecular cyclization is possible¹⁵, a highly enantioselective catalytic method has yet to be reported.

The limitations of traditional methods to achieve site- and enantioselective oxidative dearomatization led us to consider using the tools employed by nature to effect this transformation. Oxidative dearomatization has been proposed as the chirality-generating step in a number of natural product biosynthetic pathways. Enzymes capable of the dearomatization of arenes through dihydroxylation or oxidative ring cleavage have been known for decades, but the proteins responsible for oxidative dearomatization of phenols to generate *ortho*-quinol products, such as **2**, have

remained more elusive¹⁶. Only recently have *in vivo* and *in vitro* studies identified enzymes responsible for mediating oxidative dearomatization of phenolic compounds to form *ortho*-quinol products in a handful of natural product pathways¹⁷. We reasoned that these flavin adenine dinucleotide (FAD)-dependent monooxygenases represent ideal catalysts for oxidative dearomatization reactions, particularly as they require only molecular oxygen and a nicotinamide cofactor to enable catalysis under mild reaction conditions, with high site- and enantioselectivity¹⁸.

To harness the advantages offered by FAD-dependent monooxygenases, the challenges classically associated with biocatalysts, including limited substrate scope and the ability to achieve the desired selectivity, must be overcome¹⁹. A common strategy in biocatalyst development involves: (1) first selecting a single enzyme; (2) evaluating its substrate scope, site- or enantioselectivity; and then (3) engineering the protein to operate on a different suite of compounds or with altered selectivity²⁰. Given the diversity that nature has evolved in the context of natural product biosynthetic pathways, we hypothesized that greater synthetic utility could be accessed by profiling the substrate promiscuity and selectivity of a number of different FAD-dependent monooxygenases capable of catalysing the oxidative dearomatization of phenol and resorcinol substrates.

Our initial studies focused on a set of enzymes with orthogonal site- and stereoselectivities. We were guided by the work of the Cox^{17,21}, Tang²² and Watanabe²³ groups, which have each biochemically characterized FAD-dependent monooxygenases that mediate the oxidative dearomatization of resorcinol substrates to *ortho*-quinol products that are further elaborated into various classes of natural products by downstream biosynthetic enzymes (Fig. 1d). Cox and co-workers first demonstrated this transformation through *in vitro* characterization of a FAD-dependent monooxygenase, TropB, included in the gene cluster that encodes for the fungal tropolone natural product stipitonic acid (**16**). TropB catalyses the site- and stereoselective oxidative dearomatization of resorcinol **14** to alcohol **15** (Fig. 2). Also in 2012, Tang identified a similar FAD-dependent monooxygenase from a silent *Aspergillus*

¹Department of Chemistry, University of Michigan, Ann Arbor, Michigan 48109, USA. ²Life Sciences Institute, University of Michigan, Ann Arbor, Michigan 48109, USA. ³Program in Chemical Biology, University of Michigan, Ann Arbor, Michigan 48109, USA. *e-mail: arhardin@umich.edu

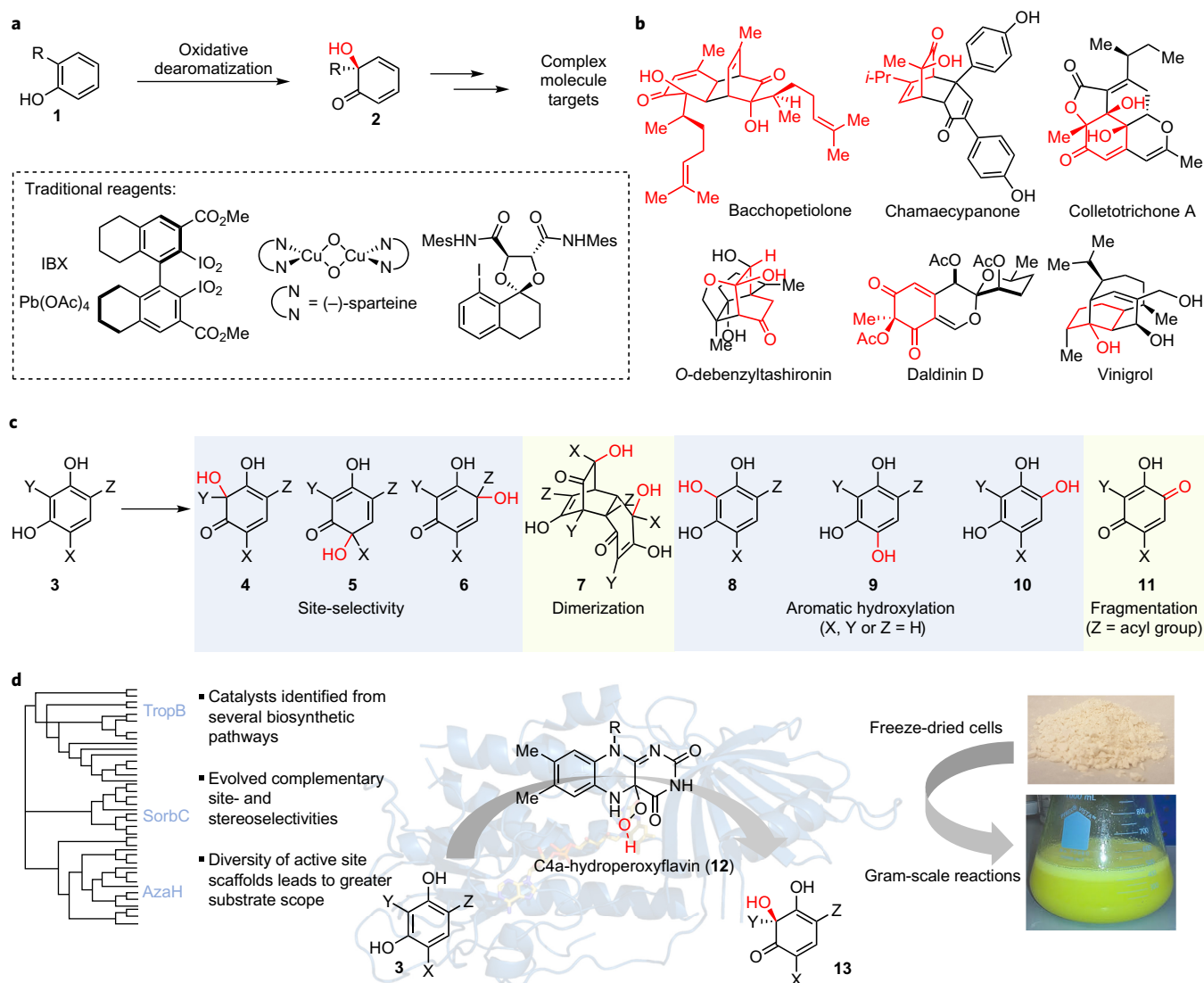


Figure 1 | Strategies for oxidative dearomatization of phenolic compounds and application in complex molecule synthesis. **a**, Oxidative dearomatization of phenolic substrates to afford *ortho*-quinol products and small-molecule reagents used for this transformation. IBX, 2-iodoxybenzoic acid. **b**, Natural products accessible from *ortho*-quinol intermediates. **c**, Potential products afforded by conditions for resorcinol oxidative dearomatization including potential product isomers, dimers and undesired products. **d**, Biocatalytic oxidative dearomatization leveraging the diversity of a suite of flavin-dependent monooxygenases from natural product biosynthetic pathways. The protein structure shown is a homology model of TropB based on the structure of Protein Data Bank ID 2DKH using the Phyre2 server.

niger ATCC 1015 gene cluster and demonstrated the role of this enzyme, AzaH, in the site-selective oxidative dearomatization of resorcinol substrate **17** to afford **18** with unknown configuration at the newly formed stereocentre. While TropB and AzaH operate with the same site-selectivity, a third enzyme in this class, SorbC, has evolved orthogonal site- and facial selectivity within the sorbicillactone A (**22**) pathway, oxidizing sorbicillin (**20**) to the C5-hydroxylation product **21**²⁴.

We began by synthesizing the native substrates for TropB, AzaH and SorbC (**14**, **17**, and **20**, respectively), which were subsequently used as positive controls for the activity of each FAD-dependent monooxygenase (see Supplementary Section III ‘Biocatalytic reactions’ for details). In parallel, the three proteins were heterologously expressed in *Escherichia coli* and purified using standard Ni-affinity chromatography. Analytical-scale *in vitro* reactions with each enzyme and the corresponding native substrate confirmed productive catalysis. In the case of TropB, we observed complete consumption of the starting material in 1 h, which corresponds to

1,000 turnovers of the catalyst (Table 1, entry I). Partial conversions were seen in the analogous assays for AzaH and SorbC, with total turnover numbers (TTNs) of 725 and 816, respectively (entries XVII and XXIX).

With activity on the natural substrates benchmarked, we next assessed the reactivity of each monooxygenase on a panel of compounds designed to probe the steric and electronic requirements of a substrate for productive catalysis. As shown in Table 1, each enzyme demonstrated a unique footprint of substrate scope. For example, TropB can tolerate an *n*-butyl ketone in place of the C1 aldehyde present in the native substrate (entries II and VIII–X), but a benzoyl substituent was not compatible (Supplementary Fig. 55). In contrast, SorbC exhibited the highest TTNs on ketone substrates with butyl or pentyl substituents that mirror the native SorbC substrate (**20**) (entries VIII, X, XXVI and XXVIII–XXXIII). AzaH demonstrated the most flexibility in the carbonyl substituent, operating with TTNs exceeding 250 for a range of aldehyde and ketone substrates (entries I, IV, V, XI–XIII, XVII–XXI, XXVII, XXVIII and XXX–XXXIII).

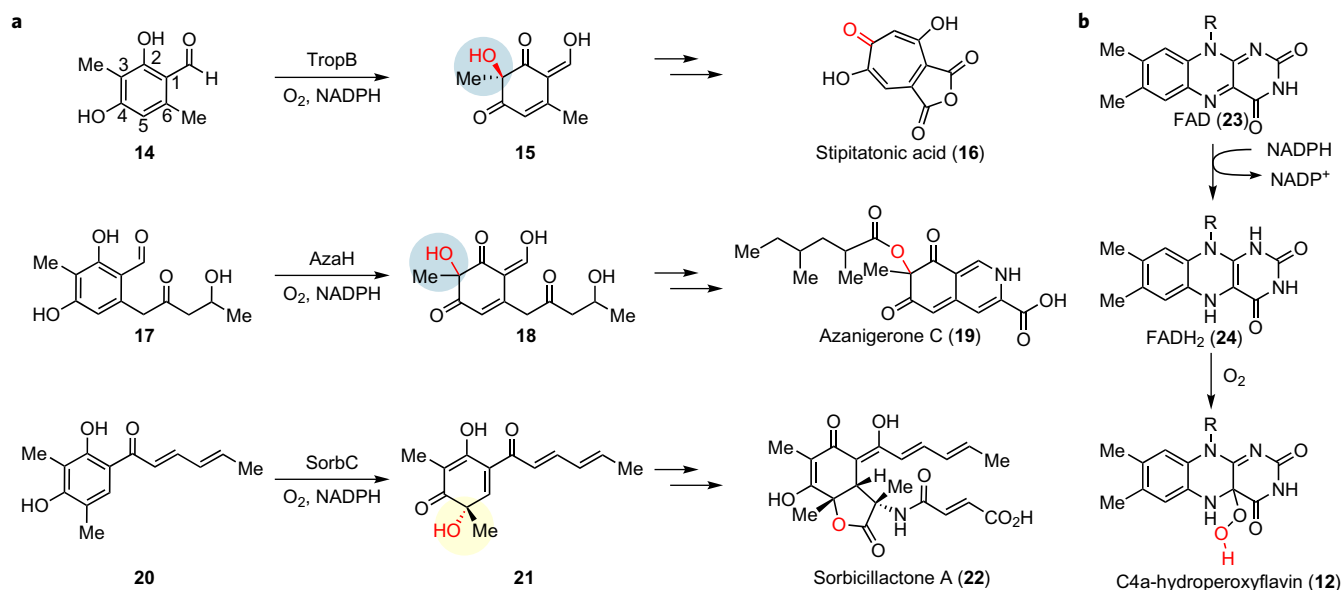


Figure 2 | Nature's tools for oxidative dearomatization of resorcinol compounds. **a**, Secondary metabolite pathways containing FAD-dependent monooxygenases that mediate the oxidative dearomatization of resorcinol substrates with orthogonal selectivities including the biosynthetic pathways to stipitonic acid (**16**), azanigerone C (**19**) and sorbicillactone A (**22**). **b**, Generation of C4a-hydroperoxyflavin (**12**) from FAD (**23**) through NADPH reduction of FAD (**23**) to FADH₂ (**24**) and subsequent oxidation to **12**.

Variation of the substitution pattern on the aryl ring was also tolerated. In the case of TropB, substrates lacking substituents at the C5 and C6 positions (entries **III** and **VII**) were converted to dearomatized products with TTNs approaching those observed with the native substrate, but AzaH and SorbC both required at least one substituent at either C5 or C6. The more sterically demanding biaryl and 6,7-bicyclic substrates were converted to dearomatized products by both TropB and AzaH (entries **XI** and **VI**).

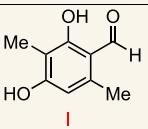
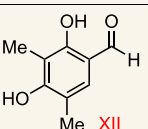
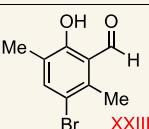
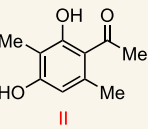
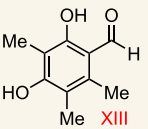
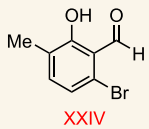
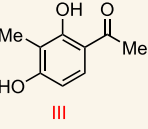
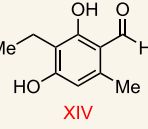
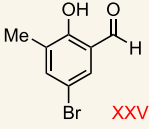
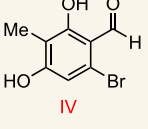
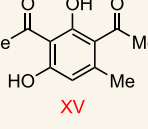
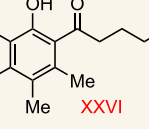
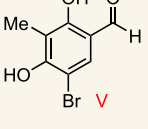
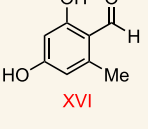
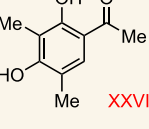
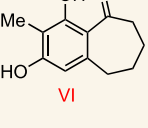
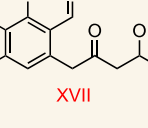
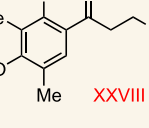
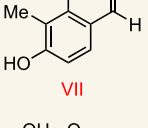
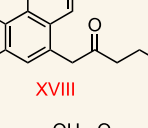
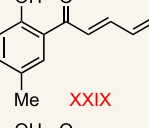
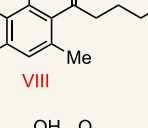
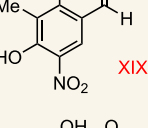
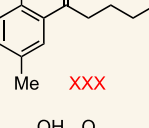
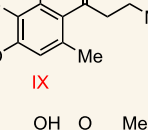
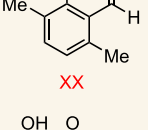
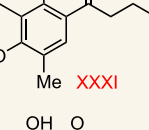
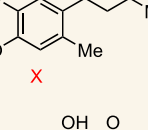
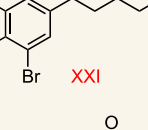
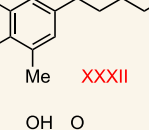
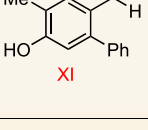
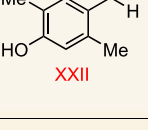
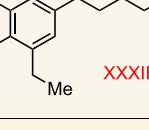
These transformations are anticipated to proceed through nucleophilic attack of the electron-rich phenol substrate onto the hydroperoxyflavin cofactor (**12**), so we were interested in evaluating more electron-poor substrates with the three FAD-dependent monooxygenases. Interestingly, brominated substrates (entries **IV** and **V**) were dearomatized by TropB and AzaH. However, even the bromine-containing substrate that meets the steric preferences of SorbC showed no detectable conversion to oxidized product with SorbC, but was hydroxylated by AzaH (entry **XXI**). AzaH was the only monooxygenase, of the three tested, with the ability to perform an oxidative dearomatization on even less electron-rich substrates such as a nitroresorcinol compound (entry **XIX**) and monophenols (entries **XX** and **XXII**). These results prompted us to examine additional monophenol substrates (entries **XXIII–XXV**). AzaH catalysed the oxidative dearomatization of brominated monophenols with low turnover numbers. Although the origin of this reactivity difference between AzaH and the other two monooxygenases is unclear, these results highlight the advantage of our approach of concurrently examining similar enzymes, which has allowed for the rapid identification of a promising general biocatalyst for the asymmetric transformation of phenols into *ortho*-quinols.

As a first step towards evaluating the selectivity and scalability of this oxidative dearomatization, substrates with the highest TTNs were selected for milligram-scale reactions. Based on the robust expression of these monooxygenases (>100 mg protein per litre of *E. coli* culture), purified protein was used in these reactions. A nicotinamide adenine dinucleotide phosphate (NADPH) recycling system was used to reduce cofactor cost²⁵. As shown in Table 2, these conditions led to the efficient transformation of substrates to dearomatized products with conversions mirroring

those observed for initial analytical-scale reactions. In some cases with excellent conversions of starting material to product, the isolated yields do not mirror these conversions. In these instances, the mass balance can be accounted for as the product dimer arising through [4+2] cycloaddition, which occurs upon concentration of the isolated product. Characterization of products from these reactions provided information on the site- and stereo-selectivity of each enzyme. Operating on their natural substrates, both TropB and AzaH selectively hydroxylate the C3 position (**15** and **36**, Table 2). This site-selectivity is conserved across a panel of unnatural substrates (Table 2 top and middle, TropB and AzaH products). Even in cases where the substrate bears a substituent at C5, the preference for C3 hydroxylation is maintained (**28** and **35**, Table 2). In contrast, SorbC demonstrates orthogonal site-selectivity, exclusively hydroxylating at C5 across the library of phenols (Table 2 bottom, SorbC products).

With their native substrates, both TropB and SorbC deliver the expected product in >99% e.e. (Table 2). The configuration of the two stereocentres present in the native AzaH product **36** was previously unknown. Therefore, racemic **17** was synthesized and presented to AzaH. Both enantiomers of **17** were converted to azaphilone product **36** to afford a 1:1 mixture of diastereomers each formed in >99% e.e. Without knowledge of the absolute configuration at C3 of azaphilone products from the *aza* gene cluster, we compared the products of TropB and AzaH with a common substrate **14**. Both enzymes gave rise to the same stereoisomer, providing evidence that AzaH installs a hydroxyl group to generate (*R*)-C3 products. Analysis of TropB and AzaH reactions with a range of unnatural substrates indicates that a high level of stereoselectivity is maintained with product e.e. values typically >99%. These results can be compared favourably to the state-of-the-art copper-oxo-sparteine oxidant developed by Porco and co-workers, which, when used superstoichiometrically, delivers *o*-quinols from resorcinol precursors in up to 98% e.e. values⁴. SorbC displays altered facial selectivity producing (*S*)-C5 products (Table 2). Excellent stereoselectivity is observed in all cases examined, except when the C3 methyl group is replaced with an ethyl group, or the carbonyl substituent is shortened to a butyl chain, eroding the stereoselectivity to deliver **40** and **43** in 94% and 95% e.e., respectively. Notably,

Table 1 | Promiscuity profile substrate scope of FAD-dependent monooxygenases TropB, AzaH and SorbC.

Substrate	Total turnover number			Substrate	Total turnover number			Substrate	Total turnover number		
	TropB	AzaH	SorbC		TropB	AzaH	SorbC		TropB	AzaH	SorbC
 I	1,000	296	0	 XII	377	385	371	 XXIII	0	49	0
 II	1,000	0	0	 XIII	432	261	0	 XXIV	0	13	0
 III	1,000	0	0	 XIV	793	0	0	 XXV	0	28	0
 IV	1,000	1,000	0	 XV	100	0	0	 XXVI	0	16	68
 V	1,000	534	0	 XVI	402	0	0	 XXVII	0	329	383
 VI	976	78	0	 XVII	0	725	0	 XXVIII	0	277	646
 VII	934	0	0	 XVIII	0	639	0	 XXIX	0	93	816
 VIII	787	0	479	 XIX	0	678	0	 XXX	0	308	656
 IX	829	0	0	 XX	0	632	0	 XXXI	0	841	858
 X	669	0	331	 XXI	0	284	0	 XXXII	0	418	889
 XI	646	542	0	 XXII	0	16	0	 XXXIII	0	639	919

Values given are total turnover numbers (TTNs) of each enzyme/substrate pair. Complete conversion of substrate to dearomatized product: TTN = 1,000 (dark green). No observed conversion of starting material is represented by 0 (light grey). Reaction conditions: 2.5 mM substrate, 2.5 μ M FAD-dependent monooxygenase, 1 mM NADP⁺, 5 mM glucose-6-phosphate (G6P), 1 U ml⁻¹ glucose-6-phosphate dehydrogenase (G6PDH), 50 mM potassium phosphate buffer, pH 8.0, 30 °C, 1 h. TTN was assessed by quantifying the remaining substrate after 1 h by UPLC, where the area of the substrate peak was divided by the area of the internal standard and compared to a substrate standard curve prepared with the internal standard.

Table 2 | Isolation and characterization of *ortho*-quinol products from reactions with TropB, AzaH and SorbC.

<p>TropB products:</p> <div> <div> <p>15</p> <p>>99% conversion 56% isolated yield >99% e.e. IBX: 20% yield</p> </div> <div> <p>27</p> <p>82% conversion 39% isolated yield >99% e.e. IBX: 14% yield</p> </div> <div> <p>28</p> <p>38% conversion 24% isolated yield 98% e.e. IBX: 31% yield</p> </div> <div> <p>29</p> <p>54% conversion 26% isolated yield >99% e.e. IBX: 18% yield</p> </div> <div> <p>30</p> <p>87% conversion 24% isolated yield >99% e.e. IBX: 17% yield</p> </div> <div> <p>31</p> <p>84% conversion 68% isolated yield IBX: 11% yield</p> </div> <div> <p>32</p> <p>73% conversion 58% isolated yield IBX: 12% yield</p> </div> <div> <p>33</p> <p>>99% conversion 93% isolated yield IBX: 13% yield</p> </div> <div> <p>34</p> <p>>99% conversion 93% isolated yield IBX: 13% yield</p> </div> </div>	
<p>AzaH products:</p> <div> <div> <p>15</p> <p>86% conversion 46% isolated yield >99% e.e. IBX: 20% yield</p> </div> <div> <p>35</p> <p>99% conversion 24% isolated yield IBX: 0% yield</p> </div> <div> <p>29</p> <p>33% conversion 19% isolated yield >99% e.e. IBX: 18% yield</p> </div> <div> <p>36</p> <p>>99% conversion 55% isolated yield 1:1 d.r.; >99% e.e. IBX: 44% yield</p> </div> <div> <p>37</p> <p>>99% conversion 82% isolated yield >99% e.e. IBX: 71% yield</p> </div> </div>	
<p>SorbC products:</p> <div> <div> <p>38</p> <p>82% conversion 43% isolated yield >99% e.e. Pb(OAc)₄: 20% yield</p> </div> <div> <p>39</p> <p>R = Me: 70% conversion 24% isolated yield >99% e.e. Pb(OAc)₄: 23% yield</p> </div> <div> <p>40</p> <p>R = Et: 50% conversion 8% isolated yield 94% e.e. Pb(OAc)₄: 8% yield</p> </div> <div> <p>41</p> <p>77% conversion 63% isolated yield 99% e.e. Pb(OAc)₄: 10% yield</p> </div> <div> <p>42</p> <p>56% conversion 27% isolated yield >99% e.e. Pb(OAc)₄: 17% yield</p> </div> <div> <p>43</p> <p>64% conversion 22% isolated yield 95% e.e. Pb(OAc)₄: 18% yield</p> </div> </div>	

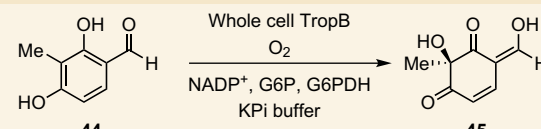
Reaction conditions: 2.5 mM substrate, 2.5 μ M FAD-dependent monooxygenase, 1 mM NADP⁺, 5 mM glucose-6-phosphate (G6P), 1 U mL⁻¹ glucose-6-phosphate dehydrogenase (G6PDH), 50 mM potassium phosphate buffer, pH 8.0, 30 °C, 1 h.

racemic **38** has been employed as a key intermediate in a number of natural product syntheses; however, no enantioselective method for accessing this class of *o*-quinols has been reported as yet. The stereochemical outcome of the biotransformation is probably controlled by the pose the substrate adopts in the enzyme active site, wherein a specific face of the substrate is presented to the hydroperoxyflavin cofactor (**12**).

In contrast, isolation of the racemic standards of these dearomatized products from traditional chemical methods employing IBX²⁶ or Pb(OAc)₄ (ref. 27) proved challenging, often affording low yields of the desired product (listed in grey, Table 2), with the mass balance accounted for as isomers, quinol dimers arising through [4+2] cycloaddition, overoxidation and product decomposition pathways. Notably, a subset of the products generated enzymatically were not accessible using standard chemical methods, including nitroquinol **35** and **45**, thus precluding the determination of the

enantioselectivity of the enzymatic transformation by comparison to racemic material. Additionally, products **31–33** were observed as a mixture of tautomers (see **33** and **34**) in a variety of solvents, which prohibited successful chiral separation and measurement of the enantiopurity of these compounds.

While enzymatic reactions are routinely carried out on sub-milligram quantities to characterize their biochemical function, the challenges associated with preparative-scale biocatalytic reactions can serve as a barrier to enzymes being embraced as tools for synthesis¹⁹. Complications with enzyme supply, labour-intensive protein purification, substrate solubility in aqueous buffer and cofactor expense can all be hurdles to preparative-scale biocatalysis. To move from milligram- to gram-scale reactions and beyond, we envisioned transitioning from *in vitro* reactions, conducted with purified protein, to a scalable platform that would be readily accessible to synthetic chemists. Toward this goal, a series of experiments using whole *E. coli*

Table 3 | Whole cell TropB reactions with wet cells versus freeze-dried cells.


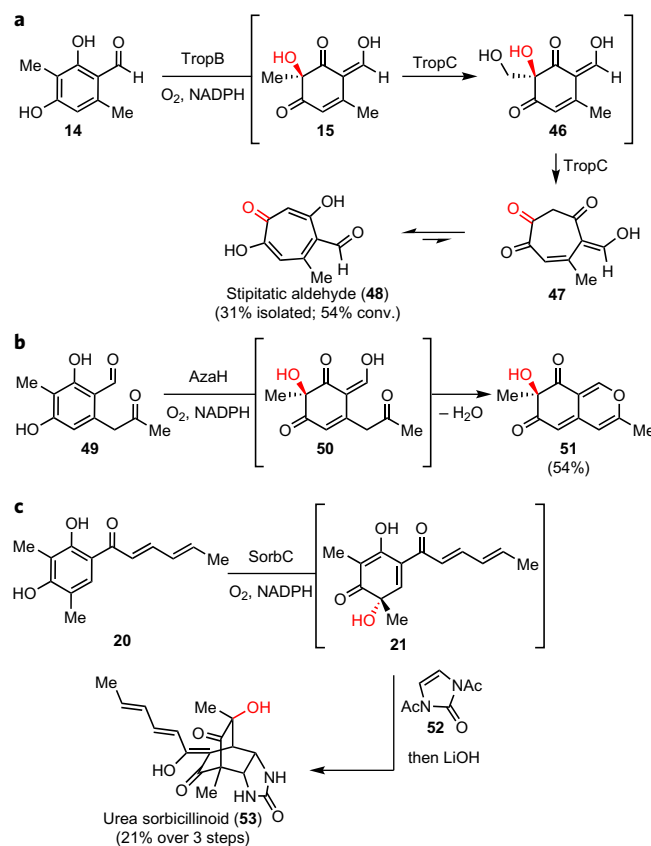
Entry	Cell preparation	Additive	% conversion
1	Wet	None	>99
2	Wet	None	>99*
3	Lyophilized	None	98
4	Lyophilized	10 wt% skim milk	83
5	Lyophilized	10 wt% sucrose	>99
6	Lyophilized	PEG 4 × 10 ³	>99

Reaction conditions: 2.5 mM substrate, 10 mg wet cell mass per ml, 1 mM NADP⁺, 5 mM glucose-6-phosphate (G6P), 1 U ml⁻¹ glucose-6-phosphate dehydrogenase (G6PDH), 50 mM potassium phosphate buffer, pH 8.0, 30 °C, 2 h. *Reaction on 1 g **44**.

cells containing heterologously expressed protein in place of purified protein was undertaken. Whole cell reactions were sufficient for complete conversion of aldehyde **44** in 2 h (Table 3, entry 1). Additionally, gram-scale reactions on a given substrate could be carried with whole cells to give comparable conversions as observed on an analytical scale. To enhance the accessibility of this method to traditional synthetic laboratories, wet whole cells were freeze-dried and stored as a lyophilized powder, which could be weighed on the benchtop and directly used in reactions without suffering a significant loss in activity compared to experiments with wet whole cells (entries 3–6). A number of excipients commonly employed to aid in the long-term stabilization of proteins were screened²⁸. When lyophilized in the presence of 10 wt% sucrose or polyethylene glycol (PEG) 4 × 10³, full activity of the enzyme was retained and the freeze-dried catalyst could be stored in the freezer at –80 °C for at least six months without any impact on reactivity.

To rapidly build molecular complexity from enzymatically generated *ortho*-quinols, we sought to leverage the reactivity of these compounds in cascade reactions by performing subsequent *in situ* enzymatic or chemical transformations. We anticipated that various natural product scaffolds could be accessed in one pot using biocatalytic dearomatization-initiated cascades. Toward this goal, we explored the synthesis of the tropolone (**48**), azaphilone (**51**) and sorbicillinoid (**53**) cores (Fig. 3). To access the tropolone natural product stipitatic aldehyde (**48**), TropB dearomatization of aldehyde **14** produced *ortho*-quinol **15**. Next, **15** was further hydroxylated by an α -ketoglutarate-dependent non-haem iron enzyme, TropC, to afford 1,2-diol **46**. Diol **46** readily underwent ring expansion in the presence of TropC to afford seven-membered ring **47**, which tautomerized to afford the tropolone, stipitatic aldehyde (**48**). Additionally, the first asymmetric synthesis of azaphilone natural product **51**³⁰ was achieved from methyl ketone **49**. Initial AzaH-mediated dearomatization delivered enol **50**, which spontaneously cyclized to the natural azaphilone **51**, which could be isolated in 54% yield and >99% e.e. Finally, urea sorbicillinoid **53** was generated directly from ketone **20** in a cascade that commenced with SorbC oxidation to deliver sorbicillinol **21**. The addition of bisacylated urea **52** led to facile [4+2] cyclo-addition. Addition of LiOH to the reaction completed the first synthesis of urea sorbicillinoid natural product **53** in 21% yield over three steps.

In summary, the results disclosed herein demonstrate the potential that FAD-dependent monooxygenases offer for site- and stereoselective oxidative dearomatization. The structural diversity available from various natural product pathways has provided a robust platform for developing a suite of biocatalysts with orthogonal selectivity and complementary substrate scope. The catalytic

**Figure 3 | One-pot cascades featuring biocatalytic oxidative**

dearomatization to access natural products. a, Stipitatic aldehyde (**48**) synthesis from aldehyde **14** through a two-enzyme cascade. **b,c**, Synthesis of natural azaphilone **51** from methyl ketone **49** (**b**) and the first synthesis of the natural product, urea sorbicillinoid **53**, through a chemoenzymatic sequence initiated by the SorbC-catalysed oxidative dearomatization of **20** (**c**).

efficiency and exquisite stereoselectivity of these catalysts paired with the mild reaction conditions provide an excellent opportunity to apply these biocatalysts in complexity-generating chemoenzymatic and multi-enzyme reaction cascades. This work provides an initial data set that will fuel the engineering of these catalysts and exploration of alternative reaction pathways.

Methods

Analytical-scale reactions. Analytical-scale reactions were performed on a 50 μ l scale. Each reaction contained 25 μ l 100 mM potassium phosphate buffer, pH 8.0, 2.5 mM substrate (2.5 μ l of a 50 mM stock solution in DMSO), 2.5 μ M FAD-dependent monooxygenase, 5 mM G6P (0.5 μ l, 500 mM), 1 mM NADP⁺ (0.5 μ l, 100 mM), 1 U ml⁻¹ G6P-DH (0.5 μ l, 100 U ml⁻¹) and Milli-Q water to a final volume of 50 μ l. The reaction was carried out at 30 °C for 1 h and quenched by the addition of 75 μ l acetonitrile with 25 mM pentamethylbenzene as an internal standard. Precipitated biomolecules were pelleted by centrifugation (16,000g, 12 min). The supernatant was analysed by ultra-high performance liquid chromatography with diode array detection (UPLC-DAD) and conversion was obtained by comparison to calibration curves of the substrate.

Whole-cell preparative-scale reactions. Whole-cell enzymatic reactions were conducted on 1 g of substrate under the following conditions: 20 weight equivalents of wet cell pellet, 5 mM substrate, 10% (vol/vol) toluene, 0.1 mM NADP⁺, 0.1 U ml⁻¹ G6PDH and 10 mM G6P for NADPH regeneration in reaction buffer (50 mM potassium phosphate buffer, pH 8.0). The reaction mixture was added to a 1 l Erlenmeyer flask and incubated at 30 °C with shaking at 100 r.p.m. After 2 h, the reaction mixture was filtered through Celite, acidified to pH 2.0 and extracted with EtOAc (3 × 500 ml). The combined organic layers were dried over sodium sulfate, filtered and concentrated under reduced pressure. The resulting mixture was purified on silica gel (MeOH/AcOH/DCM, 1:1:10) to afford the *o*-quinol product.

Data availability. Data supporting the findings of this study are available in the Supplementary Information or from the corresponding author upon request. The Supplementary Information file contains full details on the synthesis and characterization of compounds as well as the expression and purification of proteins employed in this work.

Received 31 July 2017; accepted 22 September 2017;
published online 13 November 2017

References

1. Roche, S. P. & Porco, J. A. Dearomatization strategies in the synthesis of complex natural products. *Angew. Chem. Int. Ed.* **50**, 4068–4093 (2011).
2. Wu, W. T., Zhang, L. M. & You, S. L. Catalytic asymmetric dearomatization (CADA) reactions of phenol and aniline derivatives. *Chem. Soc. Rev.* **45**, 1570–1580 (2016).
3. Volp, K. A. & Harned, A. M. Chiral aryl iodide catalysts for the enantioselective synthesis of *para*-quinols. *Chem. Commun.* **49**, 3001–3003 (2013).
4. Zhu, J. L., Grigoriadis, N. P., Lee, J. P. & Porco, J. A. Synthesis of the azaphilones using copper-mediated enantioselective oxidative dearomatization. *J. Am. Chem. Soc.* **127**, 9342–9343 (2005).
5. Bosset, C. *et al.* Asymmetric hydroxylative phenol dearomatization promoted by chiral binaphthyl and biphenylic iodonanes. *Angew. Chem. Int. Ed.* **53**, 9860–9864 (2014).
6. Wang, W. X. *et al.* Antibacterial azaphilones from an endophytic fungus, *Colletotrichum* sp. BS4. *J. Nat. Prod.* **79**, 704–710 (2016).
7. Yang, Q. L. *et al.* Evolution of an oxidative dearomatization enabled total synthesis of vinigrol. *Org. Biomol. Chem.* **12**, 330–344 (2014).
8. Shiao, H. Y., Hsieh, H. P. & Liao, C. C. First total syntheses of (±)-annuionone B and (±)-tanarifuranonol. *Org. Lett.* **10**, 449–452 (2008).
9. Nicolaou, K. C. *et al.* Biomimetic total synthesis of bisorbicillinol, bisorbibutenolide, trichodimerol, and designed analogues of the bisorbicillinoids. *J. Am. Chem. Soc.* **122**, 3071–3079 (2000).
10. Pettus, L. H., Van de Water, R. W. & Pettus, T. R. R. Synthesis of (±)-epoxysorbicillinol using a novel cyclohexa-2,5-dienone with synthetic applications to other sorbicillin derivatives. *Org. Lett.* **3**, 905–908 (2001).
11. Morrow, G. W. & Schwind, B. Synthesis of *para*-terphenyl via reductive deoxygenation of quinol derivatives. *Synth. Commun.* **25**, 269–276 (1995).
12. Schultz, A. G. & Antoulinakis, E. G. Photochemical and acid-catalyzed rearrangements of 4-carbomethoxy-4-methyl-3-(trimethylsilyl)-2,5-cyclohexadien-1-one. *J. Org. Chem.* **61**, 4555–4559 (1996).
13. Dong, S. W., Zhu, J. L. & Porco, J. A. Enantioselective synthesis of bicyclo 2.2.2 octenones using a copper-mediated oxidative dearomatization/4+2 dimerization cascade. *J. Am. Chem. Soc.* **130**, 2738–2739 (2008).
14. Sun, W. S., Li, G. F., Hong, L. & Wang, R. Asymmetric dearomatization of phenols. *Org. Biomol. Chem.* **14**, 2164–2176 (2016).
15. Uyanik, M., Yasui, T. & Ishihara, K. Hydrogen bonding and alcohol effects in asymmetric hypervalent iodine catalysis: enantioselective oxidative dearomatization of phenols. *Angew. Chem. Int. Ed.* **52**, 9215–9218 (2013).
16. Ullrich, R. & Hofrichter, M. Enzymatic hydroxylation of aromatic compounds. *Cell. Mol. Life Sci.* **64**, 271–293 (2007).
17. Davison, J. *et al.* Genetic, molecular, and biochemical basis of fungal tropolone biosynthesis. *Proc. Natl Acad. Sci. USA* **109**, 7642–7647 (2012).
18. van Berkel, W. J. H., Kamerbeek, N. M. & Fraaije, M. W. Flavoprotein monooxygenases, a diverse class of oxidative biocatalysts. *J. Biotechnol.* **124**, 670–689 (2006).
19. Khalil, A. S. & Collins, J. J. Synthetic biology: applications come of age. *Nat. Rev. Genet.* **11**, 367–379 (2010).
20. Turner, N. J. Directed evolution drives the next generation of biocatalysts. *Nat. Chem. Biol.* **5**, 568–574 (2009).
21. Abood, A. *et al.* Kinetic characterisation of the FAD-dependent monooxygenase TropB and investigation of its biotransformation potential. *RSC Adv.* **5**, 49987–49995 (2015).
22. Zabala, A. O., Xu, W., Chooi, Y. H. & Tang, Y. Characterization of a silent azaphilone gene cluster from *Aspergillus niger* ATCC 1015 reveals a hydroxylation-mediated pyran-ring formation. *Chem. Biol.* **19**, 1049–1059 (2012).
23. Sato, M. *et al.* Combinatorial generation of chemical diversity by redox enzymes in chaetoviridin biosynthesis. *Org. Lett.* **18**, 1446–1449 (2016).
24. Fahad, A. A. *et al.* Oxidative dearomatization: the key step of sorbicillinoid biosynthesis. *Chem. Sci.* **5**, 523–527 (2014).
25. Chenault, H. K. & Whitesides, G. M. Regeneration of nicotinamide cofactors for use in organic synthesis. *Appl. Biochem. Biotechnol.* **14**, 147–197 (1987).
26. Zhu, J. L., Germain, A. R. & Porco, J. A. Synthesis of azaphilones and related molecules by employing cycloisomerization of *o*-alkynylbenzaldehydes. *Angew. Chem. Int. Ed.* **43**, 1239–1243 (2004).
27. Barnes-Seeman, D. & Corey, E. J. A two-step total synthesis of the natural pentacycle trichodimerol, a novel inhibitor of TNF- α production. *Org. Lett.* **1**, 1503–1504 (1999).
28. Wessman, P., Hakansson, S., Leifer, K. & Rubino, S. Formulations for freeze-drying of bacteria and their influence on cell survival. *J. Vis. Exp.* **78**, e4058 (2013).
29. Cabrera, G. M. *et al.* A sorbicillinoid urea from an intertidal *Paecilomyces marquandii*. *J. Nat. Prod.* **69**, 1806–1808 (2006).
30. Zhang, S. P. *et al.* Antiviral anthraquinones and azaphilones produced by an endophytic fungus *Nigrospora* sp. from *Aconitum carmichaeli*. *Fitoterapia* **112**, 85–89 (2016).

Acknowledgements

This work was supported by funds from the University of Michigan Life Sciences Institute and Department of Chemistry. The authors thank Y. Tang from the University of California Los Angeles for providing a plasmid containing *azaH*. S.A.B.D. acknowledges a National Institutes of Health Chemistry Biology Interface Training Grant (T32 GM008597). A.L.L. acknowledges Graduate Assistance of Areas in National Need (GAANN P200A150164) for funding. The authors thank C. Suh and J. Liu for assistance with the synthesis of substrates.

Author contributions

S.A.B.D., A.L.L. and A.R.H.N. designed, carried out and analysed all experiments. S.A.B.D. and M.R.B. synthesized all compounds. S.A.B.D. and A.L.L. expressed and purified proteins. S.A.B.D. and A.R.H.N. wrote the manuscript, with input from all of the authors.

Additional information

Supplementary information and chemical compound information are available in the [online version of the paper](#). Reprints and permissions information is available online at www.nature.com/reprints. Publisher's note: Springer Nature remains neutral with regard to jurisdictional claims in published maps and institutional affiliations. Correspondence and requests for materials should be addressed to A.R.H.N.

Competing financial interests

The authors declare no competing financial interests.